

Activation mechanisms in sodium-doped Silicon MOSFETs

T. Fernus, R. George, N. Lumpkin, D. J. Paul, and M. Pepper

Cavendish Laboratory, University of Cambridge, J. J. Thomson Avenue, CB3 0HE, Cambridge, United Kingdom

(Dated: April 1, 2020)

We have studied the temperature dependence of the conductivity of a silicon MOSFET containing sodium ions in the oxide. The impurity band resulting from the presence of charges at the silicon-oxide interface is split into a lower and an upper band. We have observed activation of electrons from the upper band to the conduction band edge as well as from the lower to the upper band. Arguments are given in favour of the presence of Hubbard bands.

PACS numbers: 71.23.Cq, 71.55.Gs, 71.55.Jv, 72.15.Rn, 72.20.Ee, 72.80.Ng, 73.20.At, 73.40.Qv

Metal-oxide-semiconductor field effect transistors have been widely used in transport experiments because of the ability to continuously vary the electron density and the Fermi energy by use of a metal gate. This allowed Fowler and Hartstein to probe states located below the bottom of the conduction band and induced by the presence of sodium impurities in the oxide of a silicon MOSFET.^{1,2} The presence of the ions near the Si-SiO₂ interface was responsible for a subthreshold conductivity enhancement attributed to the formation of an impurity band. The temperature dependent source-drain conductivity was characterized by the existence of three parallel transport mechanisms^{3,4,5}, (i) an activation of electrons from the impurity band to the conduction band edge dominant at high temperatures, (ii) a hopping to nearest neighbour impurity levels dominant at intermediate temperatures, and (iii) a variable range hopping with $\ln T^{-1/3}$ or correlated hopping with a $\ln T^{-1/2}$ depending on the device geometry⁶ dominant at the lowest temperatures. For lower impurity concentrations, the situation is more complex as the impurity band splits into a ground and several excited bands as predicted by Gold.^{7,8} Band-to-band activation may then be observed.⁹ In a previous study¹⁰, we have observed the formation of two separate bands in sodium-doped MOSFETs when the sodium ions are drifted towards the Si-SiO₂ interface. The temperature dependence of the source-drain conductivity below $T = 20$ K was consistent with a hopping transport characterized by electron-electron interactions screened by the proximity of the metal gate. In the following sections, we will present the data obtained above 20 K. The analysis of the conductivity in temperature gives arguments for the presence of Hubbard bands.

We have processed a MOSFET in a circular geometry (Corbino) from a (100) p-silicon wafer with high resistivity ($10^4 \text{ } \Omega \cdot \text{cm}$). This geometry eliminates leakage current paths around the contacts as well as to minimize scattering with Boron acceptor impurities, especially close to the interface. The effective channel length and the interior diameter were measured to be respectively 1 μm and 110 μm . A 35 nm gate oxide was grown at 950 $^\circ\text{C}$ in a dry, chlorine-free oxygen atmosphere. Contacts were realized by implanting phosphorous at high dose and sputtering aluminium. The contact resistivity was measured to be 3.5 and 2.3 $\Omega \cdot \text{cm}^{-1}$ respectively at nitrogen and

helium temperature and the sheet resistance was 6.3 and 5.9 Ω/\square for the same temperatures. Sodium ions were introduced onto the oxide surface by immersing the device in a 10^{-7} N solution of high purity sodium chloride in de-ionised water. The surface of the chip was then dried with nitrogen gas and an aluminium gate subsequently evaporated. The application of a positive gate voltage (+4 V at 65 $^\circ\text{C}$ for 10 mins) causes the sodium ions to drift towards the Si-SiO₂ interface while the application of a -4 V DC in the same conditions removes the ions from the interface. The ions are frozen at their position once the device temperature becomes lower than 150 K. Standard low-noise lock-in techniques with an amplifier of 10^6 V/A were used to measure the source to drain conductivity. An AC excitation of 15 μV and a frequency of 11 Hz were chosen. The DC offset of the amplifier was cut using appropriate RC filters. Finally, the gate voltage was controlled by a high resolution digital to analog converter and the temperature measured by a calibrated germanium thermometer.

Fig. 1 represents the source-drain conductivity obtained at 300 mK showing the two impurity bands as well as a soft gap. This will be used as a guide for the position of the bands in the following discussion. The conductivity (T) is plotted in Fig. 2 using Miller-Abraham's model¹¹ for which the exponential prefactor is inversely proportional to the temperature. Other dependences in temperature have been used for the prefactor but did not give straight lines in the Arrhenius plots. Small polarons give also rise to such a prefactor in the mobility in the adiabatic regime, where electrons hop without introducing further deformation.^{12,13} The highest temperature used in our study is 100 K, well below the energy of longitudinal optical phonons in silicon. The presence of polarons is thus unlikely. This non-Arrhenius model for

(T) is widely found in glass systems.^{14,15} Above 20 K, a good agreement is found with activation laws but the situation is very different depending on the range of gate voltage studied. For $0.5 \text{ V} < V_g < 0.2 \text{ V}$, there exists two activation mechanisms, one at lower temperature characterized by an activation energy ϕ_1 and a second one at higher temperature with an energy ϕ_2 . On the contrary a single activation process with an energy ϕ_2 is found for $2.5 \text{ V} < V_g < 0.5 \text{ V}$, that is, in the region where the lower impurity band and the low-temperature soft gap

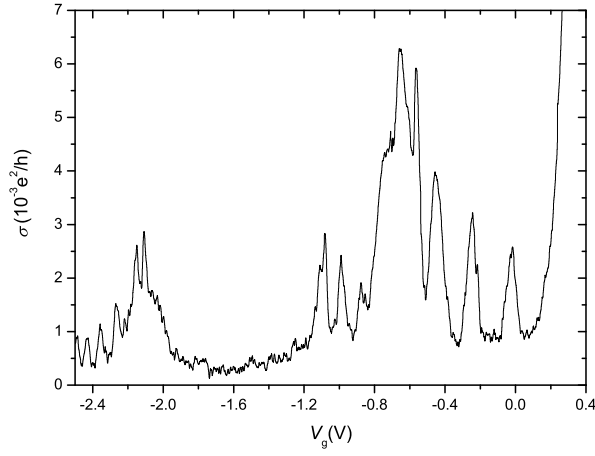


FIG. 1: Source-drain conductance versus V_g at 300 m K .

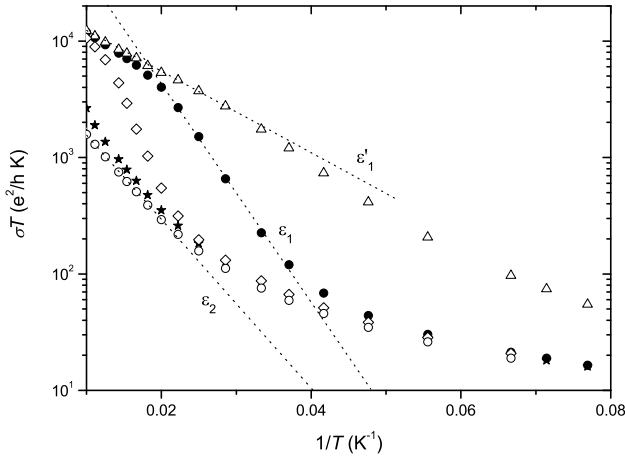


FIG. 2: Temperature dependence of the conductivity for $V_g = 0.3\text{V}$ (M), 0.15V (), 0.4V (), 0.65V (?) and 1.95V () in the activated regime. The dotted lines define the different regions of activation and their corresponding energies.

appear.

The presence of two distinct activation energies ϵ_1 and ϵ_1^0 suggest two different activation mechanisms. But contrary to Fritzsche's observations⁵ these mechanisms cannot be simultaneous because of the negative curvature of the conductivity in Fig.2 at high temperature. Consequently, the source-drain conductivity is not written as a sum of parallel processes in this region. Therefore, this suggests that the mechanism responsible for ϵ_1 may disappear at a given temperature for the benefit of the mechanism ϵ_1^0 . Fig. 3 shows the variation of the activation energy at different voltages. We observe that ϵ_1 has an exponential variation with V_g . In MOSFETs, for weak accumulation, the surface potential energy is exponentially dependent in gate voltage. The variation of $\epsilon_1(V_g)$ then simply reflects the change in the intrinsic Fermi energy and the gate capacitance when the gate voltage is varied. We can then assume that ϵ_1 corresponds to an

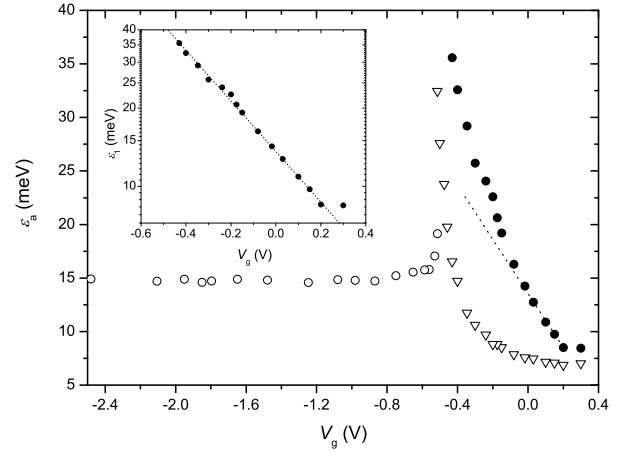


FIG. 3: Variation of the activation energy in terms of V_g for ϵ_1 (), ϵ_1^0 (O) and ϵ_2 (). The line represents the linear variation for V_g close to the threshold voltage.

activation of electrons from the upper band to the conduction band edge.³ The absence of the activation ϵ_1 for $V_g < 0.55\text{V}$ may be interpreted by the existence of a conduction band threshold in the upper band separating the localized states in the band tail from a region of conducting states at the centre of the band. The upper band edge is therefore 36 meV below the conduction band edge. Close to the threshold voltage, the variation of the activation energy with gate voltage is linear, on the first approximation. By capacitance arguments, it is possible to express the value of ϵ_1 in terms of the distance d_{Na^+} of the sodium ions from the interface :

$$\epsilon_1 = \epsilon_1^0 - e \frac{d_{Na^+}}{d_{ox}} (V_g - V_t) \quad (1)$$

where V_t is the threshold voltage.

We find that the threshold voltage for conduction in the conduction band is $V_t = 0.2\text{V}$ and that the shallowest localized states of the upper band reside at $\epsilon_1^0 = 8.5\text{meV}$ below the conduction band edge. The thickness of our oxide being d_{ox} of 35 nm, the ions may then lie as close as 0.7 nm from the Si/SiO₂ interface. This value is in a good agreement with the earlier results from Di Maria¹⁶ who obtained $d_{Na^+} = 0.5\text{nm}$ by measuring the oxide photocurrent at nitrogen temperature. We can also estimate the width of the upper impurity band tail from the energy range for which the activation process is present, giving a width close to 27 meV. Concerning ϵ_1^0 , the information obtained from the plot of the activation energy versus gate voltage is not sufficient to determine the nature of the corresponding mechanism and the variation of the pre-exponential factor with V_g (Fig. 4) needs to be analyzed.

The plot of ϵ_1^0 shows an activation law for the prefactor (Meyer-Neldel rule or MNR)¹⁷ for the all range of activation energy with a slope corresponding to a typical energy E_0 of 10.5 meV whereas the relation is highly non-

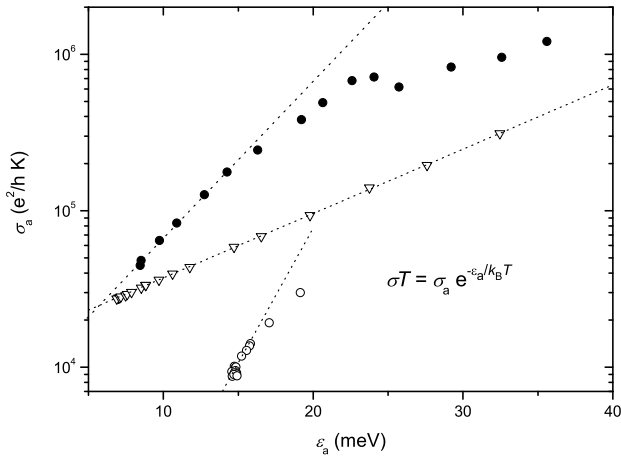


FIG. 4: Variation of the exponential prefactor in terms of the activation energy for σ_1 (\bullet), σ_1^0 (\circ) and σ_2 (\triangle).

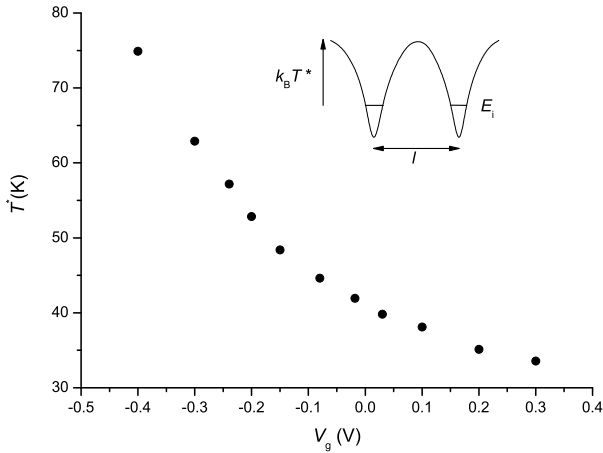


FIG. 5: Variation of the critical temperature T_c with V_g .

monotonic for σ_1 . The MNR is commonly reported in single crystal, polycrystalline, amorphous, organic semiconductors as well as ionic crystals and glasses but more generally in inhomogeneous semiconductors.^{20,21,22} Interpretations on the origin of the MNR are various but the difference in the behaviour of $\sigma_1^0(\sigma_1)$ and $\sigma_1(\sigma_1)$ makes our experimental results incompatible with a variation of the Fermi energy in temperature¹⁸ as this has been suggested. Multiphonon hopping has also been proposed¹⁹ but this would imply the absence of the MNR for $\sigma_1^0 < E_0$ which is not the case. In ionic crystal, the MNR is explained by a restructuring of the lattice formed by the ions¹⁴ and an activated conductivity due to an activation of the carrier density or of the mobility²³. In our case, an analogy could be made except that sodium ions are unlikely to move below 100 K. This has been verified by performing thermocycles from 300 mK to 100 K that modify neither the height or the position of the conductivity peaks in Fig. 1. The mechanism responsible for σ_1^0 may be interpreted in the following way. Below a certain

temperature T , sodium ions form a disordered lattice and some electrons are localised by the impurity potentials near Si-SiO_2 interface at the ion site. The effect of temperature is to thermally activate the bound electrons for conduction with an activation energy σ_1 and the plot of $\sigma_1(\sigma_1)$ gives information on the density of states. Above T , the temperature is sufficiently high to delocalise the electrons from their site allowing percolation processes to be more efficient and the scattering time to be reduced. Consequently, the conductivity is limited by scattering at the interface and thermally activated with an activation σ_1^0 . This typically describes a process of relaxation happening at the interface like those occurring in melting glasses. As a consequence, the slope of $\sigma_1^0(\sigma_1)$ may give the temperature T_g at which the glass transition occurs²⁴ and the sodium ions start moving around their positions. We find $T_g = 122$ K. The critical temperature T_c could then correspond to the necessary energy to delocalise the electrons²⁵. Fig. 5 presents the variation of T_c in terms of gate voltage. As expected, the value of T_c decreases when the electron density and the delocalization is increased.

Finally, for $V_g < -0.55$ V, the value of $\sigma_2 = 15$ m eV is nearly independent on the gate voltage except in the small transition region around -0.55 V. It is then hardly conceivable that the variation of σ_2 could be linked to any bandwidth. The average value for σ_2 is too small compared to the activation energy σ_1 to be related to an activation to the conduction band edge and it is mostly constant over the band gap. This behaviour could be explained by considering the Fermi energy for V_g below -0.55 V is pinned due to the difference in the number of states in the gap and in the band tails.²⁶ The Fermi energy then varies abruptly while decreasing negatively V_g and gets pinned in the lower band while the gate voltage is still set in the band gap region or partly in the upper band. Then, in the case of dynamic bands, the value of the activation energy may be linked to an electronic transition from the lower band to the upper band. The 15 m eV thus corresponds to a band gap. Supposing a linear relation between the gate voltage and the activation energy, it is possible to convert gate voltages into energies in the gap region at a rate of 7.7 m eV / V (Fig. 3). This activation suggests that the lower band is insulating and that the upper band has a conducting region. Consequently, in the case of sodium ions in the silicon oxide, the lower band states are fully occupied and associated with one bound electron per ion whereas the upper band states are associated with an excess electron per ion. This situation is typically found in Hubbard bands²⁷. According to the theoretical results of Bethe²⁸ on the D state (i.e. two electrons bound to a donor), an activation from the neutral state (sodium ion with a single electron) to an excited Na state is possible. Taking 11.7 for the relative permittivity of silicon as well as $0.19 m_e$ for the effective mass of electrons in silicon, we obtained $\sigma_2 = 17.8$ m eV using Bethe's formula. Nishimura²⁹ has also estimated the position of the D band correcting the initial value ob-

tained by Bethe for a single D level. Because of the formation of a band the previous value for the activation is lowered and we obtain $\phi_2 = 15\text{ meV}$ by taking the value of the localization length $\lambda = 23\text{ nm}$ measured previously on the same device¹⁰ and a density of neutral donor $N_D = 1.3 \times 10^{11}\text{ cm}^{-2}$. This value is reasonable knowing the average density of donor estimated from the threshold voltage shift gives $N_D = 3.7 \times 10^{11}\text{ cm}^{-2}$. Using Nishinura's estimate, we also found the upper states in the D band are 3.9 meV below the conduction band. This value has to be compared with the 8.5 meV found for ϕ_1 at the threshold voltage. The difference gives typically the position in energy of the conduction band edge relatively to the bottom of the conduction band. In order to bring further arguments in support of the existence of a D band, it is necessary to give an estimate of the value of the Hubbard gap U using the same method than Schiut but in two dimensions³⁰:

$$U = \frac{e^2}{4\epsilon_0\lambda} \quad (2)$$

where λ is the localization length.

The value of the localization length as well as its variation in gate voltage was calculated for the same device under the same experimental conditions.¹⁰ Below $V_g = 0.5\text{ V}$, $\lambda = 22.5 \pm 0.7\text{ nm}$ and the on-site repulsion energy is $U = 5.2\text{ meV}$. Using the conversion rate between gate voltages and energies found previously, this energy corresponds to a difference of 0.67 V in the gate voltage. This corresponds to the existing soft gap be-

tween $V_g = 1.9\text{ V}$ and $V_g = 1.2\text{ V}$ in Fig. 1. We can now check the validity of our assumptions by calculating independently the value of the Hubbard gap. For sufficiently low electron density, T and T_g are expected to have similar values. The Hubbard gap corresponding to the energy necessary to put a second electron on the same site, that is $E_0 + U$. We find a value of 15.7 meV in agreement with the value of ϕ_2 . These observations are thus compatible with the formation of Hubbard bands and a Mott-Hubbard gap formed by Coulomb interactions.

In conclusion, we have observed three main activation mechanisms in sodium-doped silicon MOSFETs at high temperature. The first one is an activation of electrons from the upper band edge to the conduction band edge. The second takes over the first one when the temperature is sufficient to delocalise electrons and corresponds to the activation of the source drain mobility. Finally, the last one has been attributed to an activation of electrons from a lower band to an upper band. The theoretical expectations for the position of the bands in energy as well as the soft gap in a case of a D band well agree with the values obtained experimentally. It is thus likely that the transport in such a localized system could be explained within the Hubbard model and that the observed upper and lower impurity bands correspond in fact to Hubbard bands.

We would like to thank Drs T. Bouchet and F. Torregrossa from Ion Beam System-France for the process in the device as well as funding from the U.S. ARDA through U.S. ARO grant number DAAD19-01-1-0552.

Electronic address: taf25@cam.ac.uk

- ¹ F. F. Fang and A. B. Fowler, Phys. Rev. 169, 619 (1967)
- ² A. Harstein and A. B. Fowler, Phys. Rev. Lett. 34, 1435 (1975)
- ³ N. F. Mott, Nobel Lecture (1977); J. Phys. C: Solid State Phys. 13, 5433 (1980)
- ⁴ A. L. Efros, N. V. Lien and B. I. Shklovskii, J. Phys. C: Solid State Phys. 12, 1869 (1979)
- ⁵ H. Fritzsche, Phys. Rev. 99, 406 (1955)
- ⁶ A. B. Fowler, A. Harstein and R. A. Webb, Phys. Rev. Lett. 48, 196 (1982)
- ⁷ C. Erginsoy, Phys. Rev. 80, 1104 (1950)
- ⁸ A. Gold and A. Ghazali, Phys. Rev. B 49, 16480 (1993)
- ⁹ H. Fritzsche, J. Phys. Chem. Solids 6, 69 (1958)
- ¹⁰ T. Fernus et al, cond-mat/0510145 (2005), to be published in Phys. Rev. B
- ¹¹ A. Miller and E. Abraham, Phys. Rev. 120, 745 (1960)
- ¹² D. Emin and T. Holstein, Ann. Phys., New-York 53, 439 (1969)
- ¹³ I. G. Austin and N. F. Mott, Adv. Phys. 18, 41 (1969)
- ¹⁴ J. Kins and S. W. Martin, Phys. Rev. Lett. 76, 70 (1996)
- ¹⁵ E. Sunyer, P. Jund and R. Jullien, J. Phys.: Cond. Matter 15, L1659 (2003)
- ¹⁶ D. J. Dimaia, J. Appl. Phys. 48, 5149 (1977)
- ¹⁷ W. Meyer et H. Nadel, Z. Tech. Phys. 12, 588 (1937)
- ¹⁸ C. Popescu and T. Stoica, Phys. Rev. B 46, 15063 (1992)
- ¹⁹ A. Yelon and B. Movaghar, Phys. Rev. Lett. 65, 618 (1990)
- ²⁰ G. G. Roberts, J. Phys. C: Solid State Phys. 4, 3167 (1971)
- ²¹ D. E. Carlson and C. R. Wronski, Amorphous Semiconductor, topics in Applied Physics, Vol 36, Ed M. H. Brodsky (New-York: Springer), p 287 (1979)
- ²² T. Dasdale and R. J. Brooks, Solid State Ionic 8, 297 (1983)
- ²³ M. Pepper, Phil. Mag. 38, 515 (1978)
- ²⁴ J. C. Dyre, J. Phys. C: Solid State Phys. 19, 5655 (1986)
- ²⁵ S. W. Martin, J. Am. Ceram. Soc. 71, 438 (1988)
- ²⁶ D. Adler and E. J. Yo, Phys. Rev. Lett. 36, 1197 (1976)
- ²⁷ P. Norton, Phys. Rev. Lett. 37, 164 (1976)
- ²⁸ H. A. Bethe and E. E. Salpeter, Quantum Mechanics of One and Two-Electron Atoms, Academic Press Inc, New-York (1957)
- ²⁹ H. Nishinura, Phys. Rev. 138, A 815 (1965)
- ³⁰ L. I. Schi, Quantum Mechanics, McGraw-Hill, New-York, 3rd Ed. (1968)